



Cost-Effective Manufacturing of Microfluidics Through the Utilization of Direct Ink Writing

Stefanus H. Prajitna¹, Christian Harito^{1*}, Brian Yulianto²

¹ Industrial Engineering Department, BINUS Graduate Program-Master of Industrial Engineering, Bina Nusantara University, Jakarta 11480, Indonesia.

² Advanced Functional Material Laboratory, Engineering Physics Department, Institut Teknologi Bandung, Jl. Ganesha, 10, Bandung 40132, Indonesia.

Abstract

Microfluidics is essential for precise manipulation of fluids in small channels. However, conventional manufacturing processes for microfluidic devices are expensive, time-consuming, and require specialized equipment in a clean room. While recent studies have improved the cost-effectiveness of this device, there is still a need for further advancement in cost efficiency. Therefore, this study aimed to develop a custom-built direct-ink writing (DIW) printer for manufacturing microfluidic devices that is more affordable. Custom-built DIW directly printed microfluidic channels onto microscope slide glass using RTV (Room Temperature Vulcanizing) silicone sealant. To finish the microfluidics manufacturing, the printed channel will be assembled by placing the same glass on top of the printed layer. This method eliminated the need for polydimethylsiloxane (PDMS) molds and casting processes that were still found in recent studies. This innovative \$250 (USD) custom-built DIW method takes 15 seconds to print microfluidics channels and showed a significant cost reduction, with each microfluidics device costing only \$0.071 (USD) compared to \$0.90 (USD) in previous studies. This study makes microfluidics more affordable and accessible for biomedical use.

Keywords:

Microfluidics; RTV Silicone; Direct Ink Writing; Particle Separation; Blood Separation; Image Processing.

Article History:

Received:	10	July	2024
Revised:	24	October	2024
Accepted:	03	December	2024
Published:	01	February	2025

1- Introduction

New methods were developed in the 1950s to create complex three-dimensional (3D) micro-patterns in semiconductors, leading to an increased interest in designing microfluidics and miniaturized systems [1]. Microfluidics is an advanced micro-technology that manipulates fluids in channels with a minimum of one dimension between 100 nm and 100 microns. The device is characterized by a compact size, which enables explorers and engineers to manipulate minimal volumes of liquids and particles. Following the discussion, the process of miniaturization offers several benefits, such as decreased usage of samples and substances, as well as improved portability [2].

Studies have shown that the conventional manufacturing procedures for the products are expensive, time-consuming, and require specialized equipment and expertise, as well as a cleanroom environment [3]. Therefore, the development of low-cost microfluidics is attracting great interest because it is promising for biomedical, particle, and cell analysis purposes, such as viruses, cancer biomarkers, blood cell separation for hematological diagnosis, and other study purposes [4–7]. In the context of the hematological examination, red blood cell (RBC) particles in healthy subjects are approximately 7 to 8.2 microns at rest and can increase up to 28 micrometers (μm) during vascularization [8, 9]. Following the discussion, microfluidic devices can be fabricated through subtractive and additive manufacturing methods. Specifically, subtractive methods include precise cutting of material using computer numerical control (CNC) machines from larger blocks of material [10]. On the other hand, additive manufacturing methods include 3D printing microfluidics, also known as 3D printing processes [11, 12].

* **CONTACT:** christian.harito@binus.ac.id

DOI: <http://dx.doi.org/10.28991/ESJ-2025-09-01-01>

© 2025 by the authors. Licensee ESJ, Italy. This is an open access article under the terms and conditions of the Creative Commons Attribution (CC-BY) license (<https://creativecommons.org/licenses/by/4.0/>).

Recent improvements show a variety of methods to improve cost and efficiency. In this study, Ayoib et al. used polydimethylsiloxane (PDMS) biopolymer and soft lithography to create cost-effective microfluidic channels with laminar fluid flow. To construct a durable mold, a master template was made with several layers of SU-8 5 and SU-8 2015 negative photoresists. Moreover, the fluid test showed no leakage during plasma oxidation, implying an efficient and cost-effective manufacturing process completion [13]. Gonçalves et al. also used stereolithography 3D printing to create microchannel molds that were combined with PDMS double casting and replica molding procedures for capillary flow studies. A PDMS microfluidics device for blood plasma separation was created using soft lithography and PDMS modified with polyethylene oxide (PEO) surfactant. Therefore, this study aimed to show that PDMS surface modification had a high potential for improving blood plasma separation efficiency in microfluidic devices by facilitating fluid flow, reducing cell aggregation, trapping air bubbles, and achieving higher levels of sample purity [14]. In comparison to other studies, Fang et al. developed a capillary flow-driven microfluidics device that proved to be an effective solution for blood plasma separation, particularly in point-of-care (POC) settings. This device used capillary action and depth filtration to separate plasma from whole blood without requiring an external power source. For instance, a study showed that the device could achieve a maximum separation efficiency of 99.8%, producing approximately 30 μL of plasma from a 200 μL blood sample [15]. Finally, Rodríguez et al. proposed the use of CO_2 laser-ablated PMMA to create microchannels for microfluidic devices based on the passive Zweifach-Fung principle. The device showed significant improvements in precision and recall for micrometer-sized particles, achieving a total accuracy of $94\% \pm 3\%$. This procedure was conducted using an economical method that did not require a clean room. In addition, the method represented a significant departure from traditional practices, leading to substantial cost savings without compromising operational effectiveness. The price of each chip was below USD 0.90, and the manufacturing process only required 15 minutes [16].

Throughout this introduction, the article begins with a review of the historical events surrounding the development of micro-patterning techniques in semiconductors and their impact on the evolution of microfluidics device technology. It then explores the fundamental principles and advantages of microfluidics, particularly in biomedical research and diagnostics. The subsequent section discusses the challenges of conventional manufacturing processes and the growing need for cost-effective alternatives. Recent advancements in microfluidics manufacturing, including soft lithography, stereolithography, and CO_2 laser ablation, are examined in detail. This article also presents a comparative analysis of various methods aimed at improving cost-effectiveness in microfluidics manufacturing devices.

Although recent studies have made significant progress in improving the cost-effectiveness of microfluidics device production, further improvements are still required to achieve even greater cost efficiency. This study proposes the use of a custom-built direct ink writing (DIW) 3D printer with a singular silicone-based polymer, such as silicone sealant. Silicone will be printed to form a microchannel wall between microscope slide glasses, effectively sealing the microchannel pattern and forming a fully enclosed microfluidics device.

2- Device Materials and Methods

The materials used in this study include silicone sealant and microscope slide glasses. Silicone sealant has exceptional adhesive properties at room temperature, vulcanizing (RTV) that was applied to a glass surface, eliminating the conventional method. Additionally, printed silicone channels were deformed to meet specific requirements by applying compressive force to the device. This process enabled the creation of narrow microchannels that functioned effectively for fluid and particle separation.

2-1- Silicone and Substrate Material

The RTV silicone sealant used in this study is a product of Sika AG Chemical, namely Sikasil-111, shown in Table 1. This type of silicone possessed several advantageous properties, such as low toxicity, excellent environmental adaptivity, resistance to degradation, and high chemical stability [17]. Moreover, sealant material was readily accessible and widely available in the market.

Table 1. Transparent silicone sealant mechanical properties

Properties	Value
Shore hardness	20-30
Tensile strength	0.5 MPa
Modulus elastic	0.35 MPa
Tensile Strain	400 %
Movement capability	25 %
Elastic recovery	80 %
Tack free time	3-10 minutes

Float glass material was used by the study to enclose the created microfluidics channels. This material referred to flat glass sheets called microscope slides glass. The investigation used float glasses as the enclosing material, which functioned as a clear and durable covering for microfluidic channels. Relating to this discussion, Table 2 [18] showed the mechanical properties of float glass. The material used met ISO 8037-1 standards, measuring 76 mm by 26 mm with a thickness of 1 mm, and it was used as both the top and bottom substrates.

Table 2. Mechanical properties of float glass

Properties	Value
Glass type	Float glass
Density	2500 kg/m ³
Compressive strength	212 MPa
Elastic modulus	70 GPa
Tensile strength	50 MPa
Impact strength	800 MPa
Vickers hardness	4.59 MPa
Poisson ratio	0.23

2-2-Method

This study used an experimental method that focused on the fabrication of microfluidic devices. Initially, a custom-built DIW printer was developed for manufacturing, which was incorporated as a tool to apply compressive force on microfluidic devices, improving the capability for fluid and particle separation. Finally, a simulation examination was conducted using a mixture of ground coffee and water to mimic cells and the fluid. This simulation also validated the performance of the microfluidics device, performed particle separation, and analyzed results using the ImageJ image processing application.

Figure 1 showed the processes of manufacturing microfluidics with a custom-built DIW printer. The process steps were to first set up the DIW printing machine with silicone sealant loaded into a syringe and a computer-aided design (CAD)-designed microfluidics channel pattern for the controller. Moreover, the printer dispensed silicone from the tip of the nozzle, emitting silicone liquid directly onto the surface of the bottom substrate that formed a pre-designed channel pattern. After printing the silicone channel wall, it was enclosed with a top substrate, thereby creating an entire microfluidics system. The next step was to drill all necessary ports, such as inlet, excess, and outlet ports.

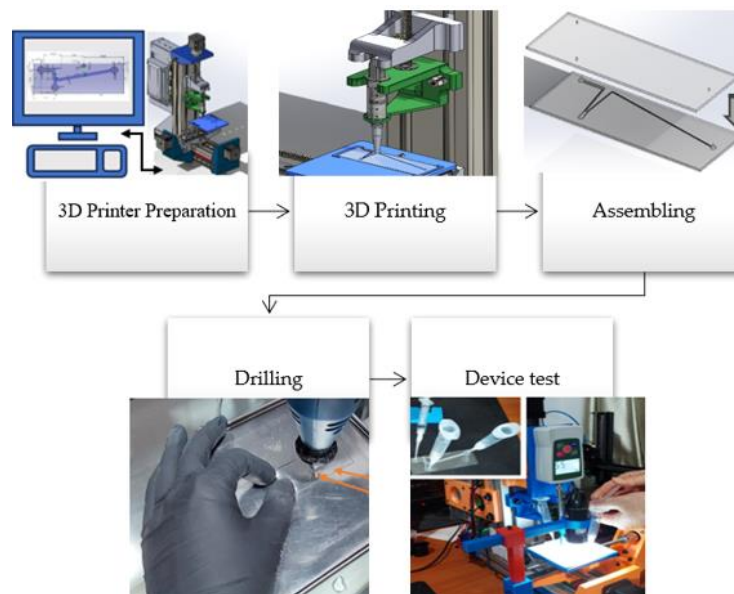


Figure 1. Study method of manufacturing cost-effective microfluidics device

The microfluidics device was finally simulated and examined by placing a digital force measurement and applying a single-point force pressure to the top substrate of the device. This force was intended to deform the silicone channel wall, leading to the narrowest channel pattern. In this condition, the force prevented certain particle dimensions from passing through the outlet port, causing the particles to travel to the excess port. During the examination, a digital microscope was placed near the pressure point to measure and record channel gap width.

Validation was carried out using ImageJ software, which analyzed the particle data collected from a digital microscope. During this process, a medical syringe was used to inject ground coffee particles mixed with water into the inlet port of the microfluidics device.

3- Result and Discussion

3-1- Custom-Built DIW Printer

The custom-built DIW printer was shown in Figure 2-A, presenting the incorporation of a digital microscope, a digital force measurement, and a syringe filled with silicone. Furthermore, the printer had a feature called Figure 2-B, which functioned as a DIW printer. This machine could print microfluidics using a loaded syringe filled with silicone sealant material. In this study, Figure 2-C showed the ability to be configured as a test and simulation tool for microfluidics devices. The printer components were mostly constructed using a fused deposition machine (FDM) that used polylactic acid (PLA) material.

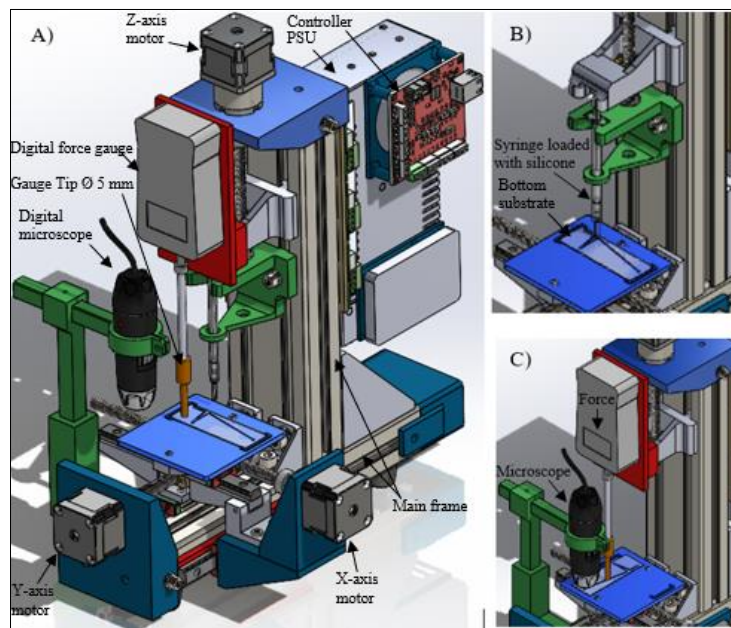


Figure 2. Custom-built DIW printer

The development of custom-built DIW printers represented an advancement in recent microfluidics manufacturing methods. Different from current methods, which require the production of molds and casting to form microfluidic channels, DIW printers directly print silicone material to create the channel patterns. This ability eliminated the need for intermediate steps, such as mold fabrication, thereby simplifying the manufacturing process, reducing material waste, and increasing general efficiency in the production of microfluidic devices. The method also simplified the process and opened up possibilities for more complex and customizable designs.

The developed DIW system was equipped with three stepper motors, one for each axis. The motors on the X and Y axes-controlled movement to form the desired design geometry, while the Z-axis motor served two functions. The primary role of the Z-axis was to drive the syringe plunger and dispense silicone sealant for printing. Additionally, the secondary role of the axis was to operate the digital force measurement along with an attached measuring tip to apply compressive force for testing and simulating microfluidic devices. These stepper motors were coordinated by a low-cost 5-axis CNC controller that executed the geometry code (G-Code) through CNC software.

Table 3 showed the specifications of the custom-built DIW printer to support the manufacturing of microfluidic devices for this study. The values showed various parameters and features designed to meet the specific requirements of microfluidics fabrication. These modifications ensured that the printer consistently and precisely produced the complicated and delicate channels required for effective microfluidic devices. Based on a travel distance of 100 mm × 100 mm, the X and Y axes were capable of moving a distance of 100 mm each. Following the distance covered by these axes, an assumption was made that the length of the float glass was 76 mm and could be used in this study. In addition, printing the perimeter of ISO 8037-1 float glass only took 6 seconds with a travel speed of up to 2000 mm/minute. This customized setup was tested and fine-tuned experimentally to achieve the best quality and performance when printing silicone material.

Table 3. Study DIW printer specification

Parameter	Dimension
Work travel X-Y axis	100 mm × 100 mm
Worktable width x length	90 mm × 90 mm
Travel speed	100 – 2000 mm/minute
Syringes	1 mL
Dispensing Flow rate	23 μ L/second
Dispensing Travel Z axes	120 mm
Axis drive	3 axis stepper motor NEMA 17
Controller	5-axis
Power Supply Unit PSU	2.5 Ampere / 1 Phase / 220 Volt
Dimension	(W) 300 mm × (L) 425 mm × (H) 420 mm
Weight	6.5 Kg

3-1-1- Printed Microfluidics Device and Cost

Figure 3 showed the DIW printing process, where silicone sealant was applied to the bottom float glass. This operation required precise coordination between silicone output and the movement of the printer worktable. The printer traveled at a speed of 1080 mm/minute, following pre-programmed directions encoded in G-Code. Concurrently, silicone was dispensed at a rate of 23 μ L/second. After extensive testing with various printing trials, this particular timing and setup was proven to be the most effective. Moreover, the setting process ensured that silicone sealant was applied evenly and precisely, producing high-quality prints.



Figure 3. DIW printing onto bottom float glass

Figure 4 showed the finished product after printing as well as assembly and accompanied by the drilled top float glass. About 1 mm diamond bit was used to drill precise ports in specific locations. These ports were essential to the operation of microfluidics devices and allowed controlled flow as well as manipulation of fluids throughout the system. In this study, Table 4 showed the processing time required for every step of the workflow by an experimentally manufactured microfluidics device.

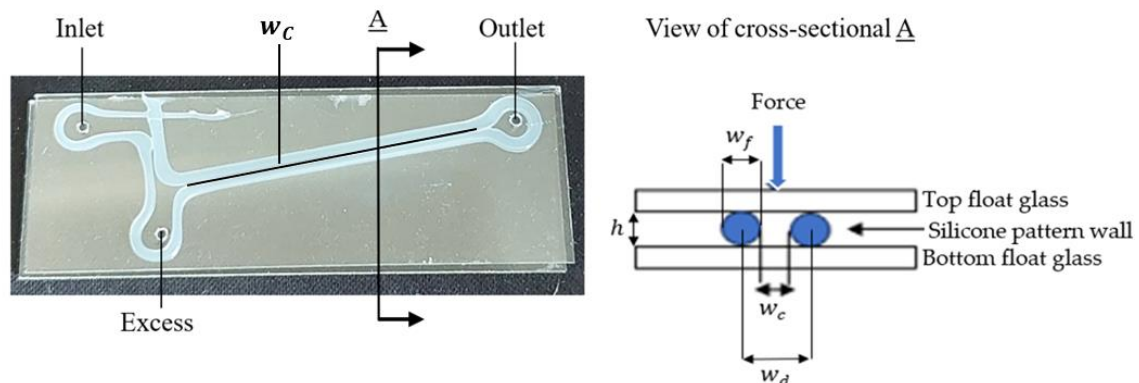


Figure 4. Printed microfluidics device

Table 4. Duration result of manufacturing microfluidics devices

Workflow	Description	Duration
3D printer preparation	Design G-code upload to printer controller with RTV silicone syringe loading onto its axis.	7 minutes
3D printing	Ongoing printing process, discharging RTV silicone onto to bottom substrate until the end of the program.	15 seconds
Assembling	Top substrate placement supported base substrate. Place the printed device at room temperature to dry off. (as shown in Table 1)	12 minutes
Drilling	All ports drilling process on to the top substrate	3 minutes
Device test	Injecting substances to simulate.	3-5 minutes

The process began by uploading G-Code from computer-aided manufacturing (CAM) design into the 3D printer controller. Subsequently, about 1 milliliter (mL) of syringe was filled with RTV silicone and attached to the mounting bracket of the axis linear actuator. After the materials and procedures were ready, the operator started printing. The syringe discharged 0.35 mL of silicone for each device in 15 seconds and then followed the programmed pattern until G-code instructions were completed. In this process, the cumulative manufacturing time for each device, including the entire workflow, was 27 minutes and 15 seconds. However, the second and third printing times were reduced by 7 minutes due to the remaining silicone in the syringe. The drying time varied depending on the silicone product used and room temperature. The drilling process was carefully conducted by immersing the dried printed device in a water pool to reduce the risk of a cracked hole. Finally, the 3D-printed microfluidics device passed through the final test to ensure that there were no leaks or breakages along the printed silicone channel wall. This examination was done by injecting clean water into the inlet port.

The budget allocated in Table 5 for the development of the experimental printer unit and production of the microfluidics device was maintained at a very low amount of \$250 (USD). The achievement of budget efficiency was accomplished by carefully selecting materials and optimizing manufacturing processes. Significantly, the manufacturing cost of a single microfluidics device was really low at \$0.071 (USD). The extraordinary cost-effectiveness of this device was due to its uncomplicated composition, consisting of only two pieces of microscope slide glass and 0.35 milliliters of silicone sealant. By optimizing these components, the production process achieved both cost-effectiveness and efficiency, presenting the possibility of manufacturing microfluidics devices at an affordable price.

Table 5. Cost outcome for the manufacturing of experimental microfluidics

Components	Description	Price (USD)
Main printer frame	Aluminum 6063T5 extrusion assembled with aluminum die-cast brackets and 12.9 class for all fasteners.	30
3D printed parts	All axis motor mounting, Axis rail mounting controller mounting, power supply unit (PSU) mounting, microscope mounting, force measurement mounting, Syringe mounting, all FDM 3D printed PLA for all axes. With 12.9 class for all fasteners.	27
Mechanical parts	Low profile ball-type linear bearing for all axes. Leadscrew T8 with coupling for all axes.	70
Electronics module	Controller, PSU, all-axis stepper motor, all-axis stepper power driver	50
microscope	Portable digital microscope.	10
Force measurement	Digital force measurement 100 N.	55
Substrate	Microscope slide glass 50 pcs.	3
Material silicone	Adhesive silicone sealant 300 mL.	5
Syringes	Syringe 1 mL 100 pcs.	3

The result of this study was comparable to the recent exploration by Rodríguez et al. [16], which achieved the fabrication of a microfluidics device in just 15 minutes using a CO₂ laser. According to Table 3, the total time required for printing to drilling microfluidics devices was approximately 15 minutes and 15 seconds, placing it close to the findings of Rodríguez et al. [16]. This process has the potential to be expedited by 3 to 5 minutes because the curing time of RTV silicone sealant is highly dependent on room temperature. Under optimal conditions, the total manufacturing time could be reduced to around 10 minutes per microfluidics device. In the context of this study, the cost of manufacturing microfluidics devices showed promising potential and offered a significant advantage compared to the \$0.90 (USD) per device in previous studies. The development of a custom-built DIW system presented a cost-effective alternative, different from commercial equipment that was usually costly. Additionally, this system reduced expenses and also enabled the production of low-cost microfluidic devices designed for particle or cell separation. By using a custom-built DIW setup, studies could achieve the desired functionality of microfluidics without relying on expensive commercial machinery. The achievement made this method highly appealing for applications that required affordability and efficiency.

3-1-2- Microfluidics Device Testing

By gradually applying force and reducing the distance between the glass substrates, it was observed that when a compressive force of 5.7 Newtons with a distance between the heights h of the glass substrates being 0.44 mm, an ideal channel width (w_c) of 0.03 mm or 30 microns was achieved. However, as the compressive forces exceeded the values in Table 6, the channel eventually collapsed and closed completely. Figure 5 showed the transformation of DIW printer into microfluidics device for testing.

Table 6. Device cross-sectional channel width w_c result

Force (N)	Width of w_c (mm)	Width of w_f (mm)	Width of w_d (mm)	Height h (mm)
1.2	0.07	1.23	1.3	0.74
3.2	0.06	1.24	1.3	0.64
4.6	0.05	1.25	1.3	0.60
5.1	0.04	1.26	1.3	0.54
5.7	0.03	1.27	1.3	0.44

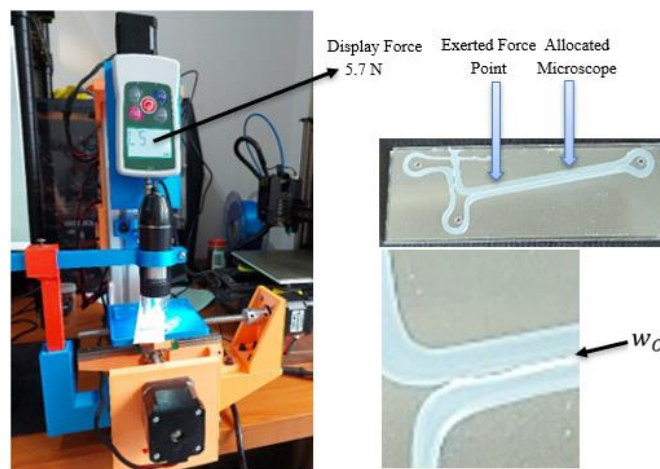


Figure 5. Microfluidics w_c measuring

The distance or width of the gap between the silicon walls w_c was very dependent on the diameter of silicon wall w_f and the distance w_d . This diameter influenced the width of w_c when compressive force was applied to microfluidics device and determined the size of the particles that passed through microfluidics channel. Moreover, the usability of the device was determined by its w_c value under compressive force. This compliance was applied to micro-particles ranging in size from 30 to 70 μm .

3-2- Microfluidics Device Validation

To validate the results of 3D printed microfluidics device, this study used a mixture of ground coffee particles with water as the fluid to flow through the device channels and the images were analyzed using image processing software. Additionally, the particle images in Figure 6 were obtained from excess as well as outlet ports and analyzed using ImageJ application with the set measurement of Feret diameter as the particle object had an irregular shape. The image processed at excess port showed larger particles and a significantly higher particle count compared to outlet port.

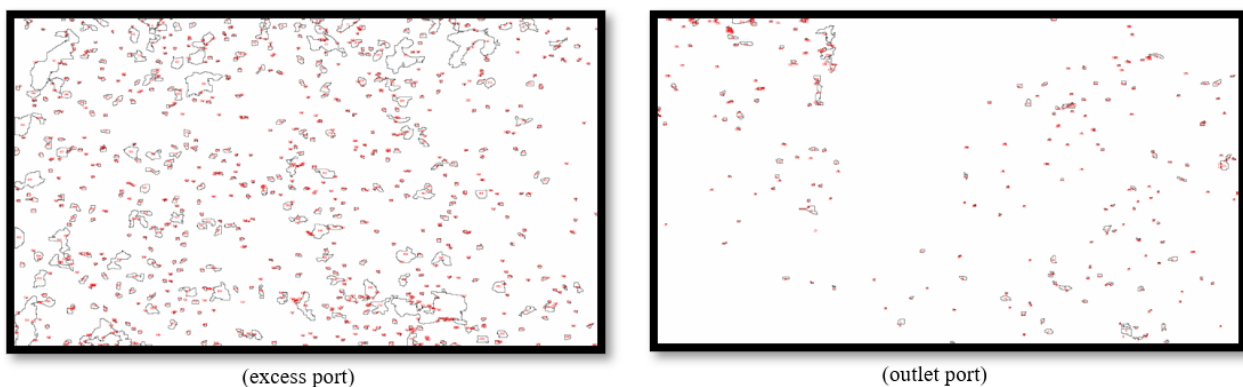


Figure 6. Particles image processing

The results of particle counting in discharge, excess, and outlet ports showed differences in size and quantity in Table 7. Excess port contained 888 particles, while outlet port contained 296. Following this discussion, the separating results were obtained with a narrowed w_c at 30 μm . Particles originating from excess port showed a larger Feret diameter of 35.3 μm , accompanied by a minimum of 19.4 μm . Moreover, the sizes that came out of outlet port were smaller, measuring 22.8 μm with a minimum diameter of 11.8 μm . The presence of larger-than-expected particles, as shown in Figures 7 and 8, was attributed to the specific conditions of the experimental setup. In Figure 7, particles with 537 μm were shown, while 8 showed size with 134 μm discharging from outlet port. This anomaly was primarily due to the height (h) being set at 0.44 mm, a value that could not be reduced further as shown in Table 5. Moreover, the observed anomaly, including larger sizes, showed a minor tolerance issue in the device. Among 296 particles analyzed, only two from outlet port were larger than expected. This minor deviation showed that the device was generally effective at separating particles to the desired specifications, even though there was some allowance for the occasional passage of larger sizes. The referral output of separation efficiency from these validation findings was described as followed:

Particle percentage from outlet port:

$$\frac{\text{Outlet port particles count}}{\text{Total n particles count}} \times 100\% = \frac{296}{1184} \times 100\% = 25\% \tag{1}$$

Table 7. Device cross-sectional channel width w_c result

Slice	Count	Feret diameter (μm)	Min. Feret diameter (μm)
Excess port	888	35.3	19.4
Outlet Port	296	22.8	11.8

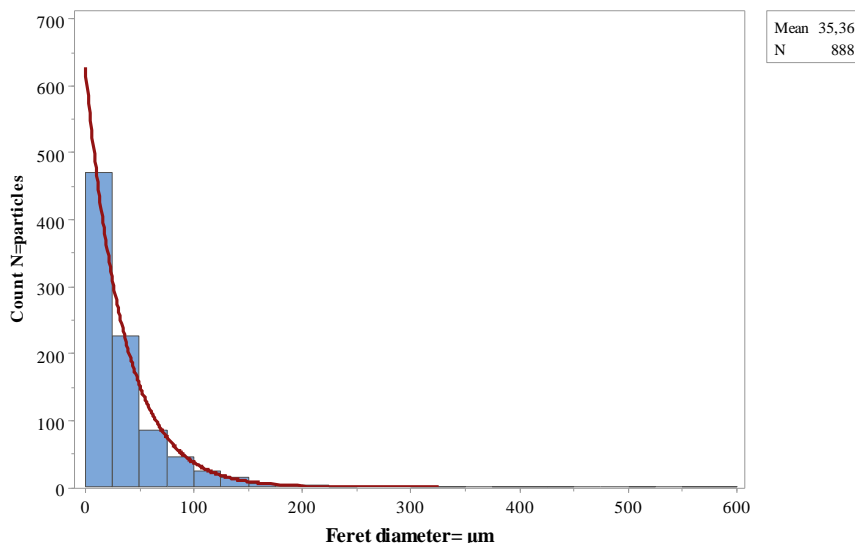


Figure 7. Particle size at excess port

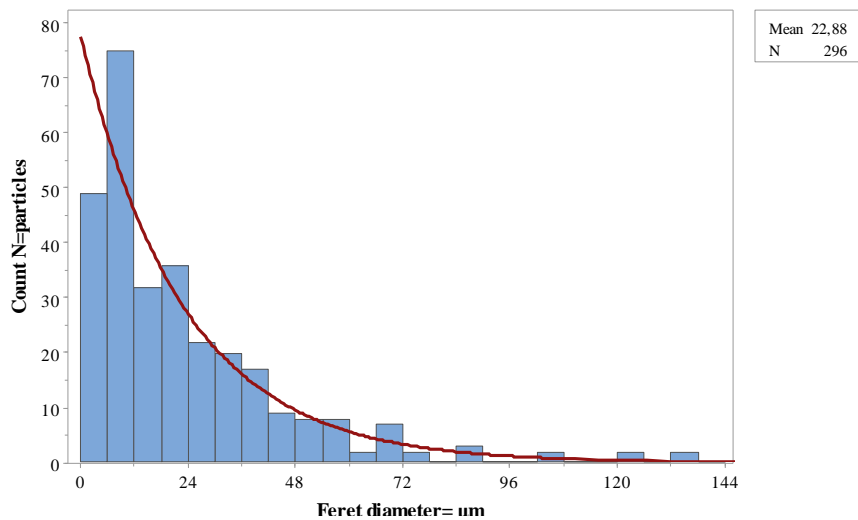


Figure 8. Particle size at outlet port

Assuming that the fluid carrying the particles was composed entirely of water. Validation showed that the fluid was 75% pure, with 25% of particle deposits present at outlet port, indicating device efficiency. Specifically, the result was 19% to 24% lower than that of recent studies by Fang et. al. [15] and Rodriguez et al. [16]. This signified that the use of an inexpensive and custom-built DIW system still produced satisfactory fluid purity efficiency.

When assessing the effect of applied force on the strength of microfluidics channels, examining both the stress on the glass and the deformation of silicone walls was important. To obtain valuable perceptions into the mechanical properties and dependability of these materials when subjected to stress, a comprehensive understanding of the magnitude of glass stress and silicone deformation was crucial. This analysis was essential in determining the impact of force-induced changes in channel width on the total performance and functionality of microfluidics systems. Accessing material resistance as a force was applied and recorded by the round tip of the digital force meter with a diameter of 5 mm, which compressed the top float glass.

$$\sigma \frac{F}{A} = \frac{5.7 \text{ N}}{\pi \cdot 2.5^2 \text{ mm}^2} = 0.290 \text{ N/mm}^2 = 0.29 \text{ MPa} \quad (2)$$

(The exerted compressive force was 0.29 MPa, which was far below the maximum allowable compressive strength of float glass 212 MPa, as shown in Table 2).

Assessing the allowable force by considering the diameter of the wall w_f of the two-channel cross-section, as shown in Figure 2.

$$A = (\pi \cdot r^2) \cdot 2 = \pi \cdot \left(\frac{1.23}{2}\right)^2 \cdot 2 = 2.376 \text{ mm}^2 = 2.4 \text{ mm}^2 \quad (3)$$

Allowable force to deform using tensile strength, as shown in Table 1 with 400% = 4 elongation at break.

$$F = \sigma \cdot A = (0.5 \text{ N/mm}^2 \cdot 4) \cdot 2.4 \text{ mm}^2 = 4.8 \text{ N} \quad (4)$$

The stress at deformed silicone wall at 5.7 N exerted force.

$$\sigma \frac{F}{A} = \frac{5.7 \text{ N}}{193.08 \cdot 1.27 \text{ mm}^2} = 0.023 \text{ N/mm}^2 = 0.023 \text{ MPa} \quad (5)$$

Even though the force exceeded the maximum allowable force which was $5.7 \text{ N} > 4.8 \text{ N}$, silicone did not break. This process was due to a small value of compressive stress in silicone channel pattern having a total length of 193.08 mm with w_f (1.27 mm) at 5.7 N, as shown in Table 4. In addition, the material had a low elongation percentage due to its mechanical properties.

Deformation allowance elongation of 400%, as shown in Table 1.

$$\Delta L = \epsilon \cdot L_0 = 4 \cdot 1.23 \text{ mm} = 4.92 \text{ mm} \quad (6)$$

Actual deformation by experimental, w_f at 1.2 N = 1.23 mm (L_0) and at 5.7 is 1.27 mm (L_1), shown in Table 4.

$$\epsilon = \frac{L_1 - L_0}{\Delta L} \cdot 100\% = \frac{1.27 - 1.23}{4.92 \text{ mm}} \cdot 100\% = 0.8 \% \quad (7)$$

The slight elongation did not affect the tensile strength of silicone wall when the force was applied. However, the cohesive strength of silicone material was due to its internal bond, which allowed it to remain intact and resist breaking when stressed [19]. The cohesive strength of silicone sealant varied, depending on the formulation and intended application. In addition, the applied force was compressive, not a shear force, and this material was intended to absorb and dissipate these stresses in its elastic range [20]. When the movement remained in the specified capability (movement capability 25%, as shown in Table 1), sealant stretched or compressed without permanent deformation or loss of bond [21]. Relating to the discussion, the material durability finding confirmed that the selected materials, silicone sealant, and float glass, were appropriate for this study.

4- Conclusion

In conclusion, although recent studies progressed in improving the cost-effectiveness of microfluidics device manufacturing, additional improvements were required to achieve greater cost efficiency. These improvements were critical to making microfluidics technology more accessible and affordable. Therefore, this study proposed a more cost-effective method to manufacture microfluidic devices by using silicone sealants and microscope glass as the primary materials that would be deformed to achieve certain specifications, as well as a custom-built DIW printer for printing directly to create a microchannel wall between microscope slide glasses.

The main equipment used in this study was a custom-built DIW printer, which was specifically designed to manufacture microfluidic devices. Additionally, the printer was equipped with a digital force meter and digital microscope. The total cost of custom-built equipment was \$250 (USD). The method was able to complete the device manufacturing process in 15 minutes, and due to the influence of room temperature caused by RTV silicone, the manufacturing process could be faster. Additionally, the deformability of the device made it capable of selectively sorting particles in a specific size range. In this particular case, the microfluidics device effectively separated and sorted particles that were between 30 and 70 μm in size, and the manufacturing cost per device was \$0.071 (USD), which was greatly affordable compared to recent studies.

In this study, ImageJ analyzed that the separation efficiency of the device sets reached 75% fluid purity after the particles were sorted through the outlet port. Despite the slightly lower efficiency from recent studies, the cost-effectiveness and accessibility of custom-built DIW systems offered a practical balance between performance and affordability. In association with biomedical studies for blood plasma separation, this device could be configured because 90% of plasma is water, which could be used for comprehensive human health examinations with a small amount of 14 μl plasma [22]. This ability made the device a decent option at a more affordable price.

4-1-Future Study

Future studies are expected to combine microfluidics and biosensor devices, particularly in improving the precision and usability of microfluidics systems, leading to more reliable and reproducible results. An important application would be in medical diagnostics, where the combination of these technologies could be used for blood separation, which allows more sensitive and specific detection of biomarkers for various diseases. In addition, the collaboration is able to improve health monitoring by providing continuous and real-time analysis. In general, the convergence of this device is expected to transform diagnostics and health monitoring.

5- Declarations

5-1-Author Contributions

Conceptualization, C.H.; methodology, C.H.; software, S.H.P.; validation, S.H.P.; formal analysis, S.H.P.; investigation, S.H.P.; resources, S.H.P.; data curation, S.H.P.; writing—original draft preparation, S.H.P.; writing—review and editing, S.H.P.; visualization, C.H.; supervision, B.Y.; project administration, C.H.; funding acquisition, C.H. All authors have read and agreed to the published version of the manuscript.

5-2-Data Availability Statement

Data sharing is not applicable to this article.

5-3-Funding

This study was funded by Direktorat Riset, Teknologi, dan Pengabdian Kepada Masyarakat, Direktorat Jendral Pendidikan Tinggi, Riset, dan Teknologi, Kementerian Pendidikan, Kebudayaan, Riset, dan Teknologi under Penelitian Tesis Magister with contract number 784/LL3/AL.04/2024.

5-4-Acknowledgements

The author is grateful to all parties that assisted in the conclusion of this study, specifically Dr. Muhammad Asrol STP., MSi. Head of Master Industrial Engineering, and BINUS Graduate Program, for indispensable mentorship, assistance, and motivation. CH is also supported by a postdoctoral program at the Advanced Functional Materials Laboratory, Department of Engineering Physics, Faculty of Industrial Technology, Institut Teknologi Bandung.

5-5-Institutional Review Board Statement

Not applicable.

5-6-Informed Consent Statement

Not applicable.

5-7-Conflicts of Interest

The authors declare that there is no conflict of interest regarding the publication of this manuscript. In addition, the ethical issues, including plagiarism, informed consent, misconduct, data fabrication and/or falsification, double publication and/or submission, and redundancies have been completely observed by the authors.

6- References

- [1] Liu, Z., Li, M., Dong, X., Ren, Z., Hu, W., & Sitti, M. (2022). Creating three-dimensional magnetic functional microdevices via molding-integrated direct laser writing. *Nature Communications*, 13(1), 2016. doi:10.1038/s41467-022-29645-2.
- [2] Convery, N., & Gadegaard, N. (2019). 30 years of microfluidics. *Micro and Nano Engineering*, 2, 76–91. doi:10.1016/j.mne.2019.01.003.
- [3] Amin, R., Knowlton, S., Hart, A., Yenilmez, B., Ghaderinezhad, F., Katebifar, S., Messina, M., Khademhosseini, A., & Tasoglu, S. (2016). 3D-printed microfluidic devices. *Biofabrication*, 8(2), 022001. doi:10.1088/1758-5090/8/2/022001.
- [4] Scott, M. D., Matthews, K., & Ma, H. (2019). Assessing the Vascular Deformability of Erythrocytes and Leukocytes: From Micropipettes to Microfluidics. *Current and Future Aspects of Nanomedicine*, IntechOpen, London, United Kingdom. doi:10.5772/intechopen.90131.
- [5] Martawidjaja, M., Yemima, S., Hananda, N., Kamul, A., Prajitna, S. H., Harito, C., & Susanto, R. (2023). 3D Printing for medical devices: Mini review and bibliometric study. *E3S Web of Conferences*, 426. doi:10.1051/e3sconf/202342601077.
- [6] Saha, S. C., Francis, I., & Nassir, T. (2022). Computational Inertial Microfluidics: Optimal Design for Particle Separation. *Fluids*, 7(9), 308. doi:10.3390/fluids7090308.
- [7] Tanjaya, H., Darius, R. A., Debora, Hananda, N., Kamul, A., Prajitna, S. H., Harito, C., & Susanto, R. (2023). A review of Microfluidic blood separation techniques. *E3S Web of Conferences*, 426. doi:10.1051/e3sconf/202342601063.
- [8] Tomaiuolo, G., Lanotte, L., D'Apolito, R., Cassinese, A., & Guido, S. (2016). Microconfined flow behavior of red blood cells by image analysis techniques. *4th Micro and Nano Flows Conference*, 7-10 September, 2014, London, United Kingdom.
- [9] Agarwal, S., Kumar, V., & Shakher, C. (2017). Analysis of red blood cell parameters by Talbot-projected fringes. *Journal of Biomedical Optics*, 22(10), 1. doi:10.1117/1.jbo.22.10.106009.
- [10] Salieb-Beugelaar, G. B., Liu, K., & Hunziker, P. (2018). Subtractive Manufacturing of Microfluidic 3D Braid Mixers. *Advanced Engineering Materials*, 20(11), 1800243. doi:10.1002/adem.201800243.
- [11] Juang, Y.-J., & Chiu, Y.-J. (2022). Fabrication of Polymer Microfluidics: An Overview. *Polymers*, 14(10), 2028. doi:10.3390/polym14102028.
- [12] Richmond, T., & Tompkins, N. (2021). 3D microfluidics in PDMS: manufacturing with 3D molding. *Microfluidics and Nanofluidics*, 25(9). doi:10.1007/s10404-021-02478-z.
- [13] Ayoib, A., Karim, N. A. A. A., Hashim, U., Shamsuddin, S. A., Abd Rahman, S. F., Fathil, M. F. M., & Parmin, N. A. (2024). Cost-Effective Fabrication of Polydimethylsiloxane (PDMS) Microfluidics for Point-of-Care Application. *International Journal of Nanoelectronics and Materials (IJNeaM)*, 17, 143–151. doi:10.58915/ijneam.v17ijune.848.
- [14] Gonçalves, M., Gonçalves, I. M., Borges, J., Faustino, V., Soares, D., Vaz, F., Minas, G., Lima, R., & Pinho, D. (2024). Polydimethylsiloxane Surface Modification of Microfluidic Devices for Blood Plasma Separation. *Polymers*, 16(10), 1416. doi:10.3390/polym16101416.
- [15] Fang, X., Sun, C., Dai, P., Xian, Z., Su, W., Zheng, C., Xing, D., Xu, X., & You, H. (2024). Capillary Force-Driven Quantitative Plasma Separation Method for Application of Whole Blood Detection Microfluidic Chip. *Micromachines*, 15(5), 619. doi:10.3390/mi15050619.
- [16] Rodríguez, C. F., Báez-Suárez, M., Muñoz-Camargo, C., Reyes, L. H., Osma, J. F., & Cruz, J. C. (2024). Zweifach-Fung Microfluidic Device for Efficient Microparticle Separation: Cost-Effective Fabrication Using CO₂ Laser-Ablated PMMA. *Micromachines*, 15(7), 932. doi:10.3390/mi15070932.
- [17] Liang, W., Ge, X., Ge, J., Li, T., Zhao, T., Chen, X., Song, Y., Cui, Y., Khan, M., Ji, J., Pang, X., & Liu, R. (2018). Reduced Graphene Oxide Embedded with MQ Silicone Resin Nano-Aggregates for Silicone Rubber Composites with Enhanced Thermal Conductivity and Mechanical Performance. *Polymers*, 10(11), 1254. doi:10.3390/polym10111254.
- [18] Sharma, A., Jain, V., & Gupta, D. (2019). Comparative analysis of chipping mechanics of float glass during rotary ultrasonic drilling and conventional drilling: For multi-shaped tools. *Machining Science and Technology*, 23(4), 547–568. doi:10.1080/10910344.2019.1575402.
- [19] Jang, Y., Nabae, H., & Suzumori, K. (2022). Effects of Surface Roughness on Direct Plasma Bonding between Silicone Rubbers Fabricated with 3D-Printed Molds. *ACS Omega*, 7(49), 45004–45013. doi:10.1021/acsomega.2c05308.
- [20] Liao, Z., Yang, J., Hossain, M., Chagnon, G., Jing, L., & Yao, X. (2021). On the stress recovery behaviour of Ecoflex silicone rubbers. *International Journal of Mechanical Sciences*, 206. doi:10.1016/j.ijmecsci.2021.106624.
- [21] van den Berg, D., Asker, D., Awad, T. S., Lavielle, N., & Hatton, B. D. (2023). Mechanical deformation of elastomer medical devices can enable microbial surface colonization. *Scientific Reports*, 13(1), 7691. doi:10.1038/s41598-023-34217-5.
- [22] Brakewood, W., Lee, K., Schneider, L., Lawandy, N., & Tripathi, A. (2022). A capillary flow-driven microfluidic device for point-of-care blood plasma separation. *Frontiers in Lab on a Chip Technologies*, 1, 1051552. doi:10.3389/frlct.2022.1051552.